ORIGINAL REPORT

# Effect on the Skin Microbiota of Oral Minocycline for Rosacea

Yiyi ZHANG[1], Ying ZHOU[2], Philippe HUMBERT[3], Dengfeng YUAN[2] and Chao YUAN[1]
[1]Department of Skin & Cosmetic Research, The Shanghai Skin Disease Hospital of Tongji Medical University, Shanghai, [2]R&D Center, Shanghai Jahwa United Co., Ltd, Shanghai, People's Republic of China and [3]University of Franche-Comté, Inserm U1098, Besançon, France

In the rosacea an unstable skin microbiota is significant for disease progression. However, data on the influence on the skin microbiota of treatment with systemic antibiotics are limited. This single-arm trial recruited patients with rosacea. Oral minocycline 50 mg was administered twice daily for 6 weeks. The lesions on the cheek and nose were sampled for 16S rRNA amplicon sequencing and metagenomic sequencing at baseline, 3 weeks and 6 weeks of treatment. Physiological parameters were detected using non-invasive instruments. After treatment, distribution of the Investigator Global Assessment scores changed significantly. For the skin microbiota, a notable increase in α-diversity and a shift of structure were observed after treatment. Treatment was accompanied by a reduction in the relative abundance of *Cutibacterium* and *Staphylococcus*, indicating negative correlations with increased bacterial metabolic pathways, such as butyrate synthesis and L-tryptophan degradation. The increased butyrate and tryptophan metabolites would be conducive to inhibiting skin inflammation and promoting skin barrier repair. In addition, the abundance of skin bacterial genes related to tetracycline resistance and multidrug resistance increased notably after antibiotic treatment.

## SIGNIFICANCE

The effect on the skin microbiota of oral minocycline for rosacea remains unclear. A single-arm trial was conducted among 36 patients with rosacea treated with oral minocycline 50 mg twice daily for 6 weeks, to assess the efficacy and safety of oral minocycline. Genetic sequencing of skin lesions on the cheeks and nose was also performed at different times during oral treatment with minocycline to investigate alterations in the diversity, structure and composition of skin microbiota. Alterations in microbial metabolism and drug resistance were observed, which might guide the clinical selection of antibiotic.

Rosacea is a common chronic inflammatory dermatitis predominantly affecting the centrofacial region, which is characterized by cutaneous features of transient or persistent centrofacial erythema and concomitant telangiectasia, papules, pustules, and phymas (rhinophyma) (1–4). The pathophysiology of rosacea remains uncertain. Recent data suggest that the skin microbiota would be involved (5, 6). Several microorganisms, including *Demodex folliculorum*, *Staphylococcus epidermidis* and *Cutibacterium acnes*, were reported as potential players in the pathogenesis of rosacea, based on their different pattern in patients with rosacea compared with healthy people (7–9). While, to date, there are no specific microbial strains conclusively linked to the development of rosacea, the improvement observed after treatment with antibiotics supports the theory that microbiota could be involved (10).

Tetracycline antibiotics, such as tetracycline, doxycycline, and minocycline, are widely used as oral therapies to control inflammatory papules/pustules of rosacea (11). Minocycline can be used to manage rosacea (12–14). Furthermore, minocycline has been shown to induce profound changes in the skin microbiota in patients with acne (15–17), but its effects on the skin microbiota in patients with rosacea are seldom reported.

Therefore, the aim of this study is to investigate the influence of minocycline on the diversity, structure, and composition of skin microbiota, as well as the development of bacterial antibiotic resistance in patients following treatment with minocycline.

## MATERIALS AND METHODS

*Study participants*

This study was a single-arm trial. Patients diagnosed with rosacea according to ROSacea COnsensus (ROSCO) 2019 (18) were enrolled between July 2021 and November 2021 at the Skin and Cosmetic Research Department of the Shanghai Skin Disease Hospital, China. The inclusion criteria were: (*i*) age ≥25 years; (*ii*) grade 3–5 rosacea based on the Investigator Global Assessment of Rosacea Severity Score (IGA-RSS); (*iii*) willingness to avoid facial washing for 12 h before skin sampling; and (*iv*) willingness to not apply topical agents to the face throughout the trial. The exclusion criteria were: (*i*) history of systemic or topical antibiotic use within 1 month of the baseline study visit; (*ii*) hypersensitivity to tetracyclines; (*iii*) systemic rosacea treatment within 4 weeks; (*iv*) topical rosacea treatment within 2 weeks; (*v*) pregnancy or lactation; or (*vi*) inability to provide informed consent. The study was approved by the Ethics Committee of Shanghai Skin Disease

Hospital (approval #2019-31). Written informed consent was obtained from each patient.

### Antibiotic treatment and sample collection

Participants were instructed to take minocycline 50 mg twice daily for 6 weeks, and to not wash their face or apply any skin care products 12 h before each visit. At baseline, week 3, and week 6, rosacea severity was evaluated by 3 physicians with equivalent credentials. Two of these physicians assessed the patients directly on-site, while the third performed evaluations using photographs captured by the VISIA skin tester (Canfield Scientific, Inc. USA). Following independent assessments, all 3 physicians convened in a consensus meeting to finalize the severity scoring. The IGA-RSS uses a 7-point numerical scale from 0 to 6 to describe rosacea symptoms [19]. Skin samples were collected from 1 side lesions of the cheek (9 cm$^2$ area) and from the nose with a single sterile cotton swab (Changde Bikeman Biotechnology Co. China).

### Physiological parameter detection

After each visit, the participants washed their entire face with tap water after sample collection and waited for 30 min under controlled conditions with an environmental temperature of 18–22°C and relative humidity of 40–60%. Transepidermal water loss (TEWL), skin surface hydration (SSH), skin pH, erythema index (EI), and (CM2600D) a* were measured.

### 16S rRNA gene V3–V4 amplicon sequencing and metagenomic sequencing

Genomic DNA was extracted from samples using the QIAamp PowerFecal Pro DNA Kit (QIAGEN, USA, 51804). For the amplicon sequencing, PCR targeting the V3–V4 region of the 16S rRNA gene with primers forward (5'-CCTACGGGNGGCWG-CAG-3') and reverse (5'-GACTACHVGGGTATCTAATCC-3') [20]. The subsequent amplicon sequencing was performed on a MiSeq platform to generate 300-bp pair-end reads (Illumina, CA, USA). For the metagenomic sequencing, library preparation was performed using the KAPA HyperPlus Library Preparation Kit (Roche, ZAF, KK8514). The size distribution of the libraries was analysed using an Agilent2100 Bioanalyzer (Agilent Technologies Inc. USA) and quantified using real-time PCR. Whole-genome shotgun sequencing was performed using the Illumina Novaseq 6000 platform (Illumina, USA) to obtain 150-bp forward and reverse pair-end reads.

### Bioinformatic analysis

The amplicon sequencing raw data was analysed using QIIME2 version 2021.4 [21]. The adapters of the original sequences were removed using the "cutadapt" plugin of QIIME2. The sequences were truncated with DADA2 and further filtered, denoised, removing the chimeras, and merged to obtain the abundance and representative sequences of amplicon sequence variants (ASVs). Representative sequences for ASVs were built into a phylogenetic tree using core-metrics-phylogenetic pipeline in QIIME2 and were assigned to taxonomy using the Silva database (release 138). All samples were randomly subsampled to equal depths of 19,928 reads before the following analysis. The α-diversity and structure of the samples were calculated by the diversity plugin of QIIME2. The structure of the microbiota was assessed by unsupervised principal coordinate analysis (PCoA) based on Bray Curtis distance [22]. PICRUST2 was used to predict the metabolic function pathways based on the MetaCyc database of skin microbiota based on the representative sequences of samples.

For the metagenomic sequencing raw data, sequence quality control and trimming of adaptors were performed using Bowtie2.4.1 and Trimmomatic v0.39. Next, quality-processed reads that did not match the hg19 human reference genome from each sample were de novo assembled into at least 500-bp scaffolds using the SOAP-denovo software v2.04. The ORF prediction for each assembled scafftigs was performed using MetaGeneMark v2.10 and filtered out the ORF less than 100 nt using default parameters. CD-HIT software v4.8.1 was used to remove the redundant sequences. The reads of genes were calculated from the comparison between the clean data and the initial gene set using SOAP2 software v2.21. The unigenes were assigned to taxonomy based on NCBI NR databases (Version 2018-01-02) using DIAMOND v0.9.9.110. Meanwhile, the unigenes were blasted to the KEGG database (version 2019.10) and assigned to the functional modules. HMMER v3.1b2 tool hmmbuild was used to train the hidden Markov model of each gene. Then hmmsearch was used to predict each gene of the butyrate synthesis pathway in the non-redundant gene sets, and the corresponding relative abundance was calculated as the final abundance result data.

### Outcomes

The primary endpoint for efficacy assessment was the proportion of individuals achieving "treatment success" (i.e. IGA-RSS grade $\leq 1$ and a $\geq 2$-grade improvement compared with baseline level) at week 6.

The secondary endpoints included the adverse events (AEs), SSH, TEWL, skin pH, EI, and (CM2600D) a*, the Shannon index, observed ASV numbers, total numbers of bacteria on the skin, amplicon sequencing data, alterations in the metabolic functions of the skin microbiota, and antibiotic resistance. Shannon index and the number of observed ASVs were indexes of α-diversity, which reflected the intra-sample diversity and richness of the skin microbiota, respectively. Participants' compliance with antibiotic treatment was initially checked, and minocycline treatment-related AEs were inquired about at every visit.

### Statistical analysis

The microbiota structure among baseline, week 3, and week 6 was compared by permutational analysis of variance test (PERMA-NOVA, 999 permutation tests) using the QIIME2 diversity plugin. For the single microbiota features, the Kolmogorov-Smirnov test was first used to test the normality. One-way analysis of variance (ANOVA) with Tukey's multiple comparisons test was used to evaluate the difference between the 3 time-points for the data with normal distribution; otherwise, the Kruskal–Wallis test with Dunn's multiple comparisons was used. These analyses were conducted and visualized using Graphpad Prism 9 (GraphPad Software, San Diego, CA, USA).

Linear discriminant analysis effect size (LEfSe) was used to determine the differential microbiota characteristics. Key genera or pathways were determined based on the differences, the statistical tests, and the frequency of the characteristic in the total population. The criteria were: (*i*) LDA score > 2 in the LEfSe model; (*ii*) frequency in the total population > 10%; (*iii*) false discovery rate (FDR)-adjusted *p*-value of the Wilcoxon rank sum test < 0.1; and (*iv*) absolute value of the log$_2$ (fold change/baseline) > 1. The heatmap of the abundance of the key genera or pathways in the population was drawn using the R software package pheatmap.

Spearman's correlation coefficients (ρ) and *p*-values of the correlations between indicators were calculated using the R package psych. The Original FDR method of Benjamini and Hochberg was used to correct the *p*-value and calculate the FDR-adjusted *p*-value. The R software package pheatmap was used to draw a heatmap of the correlation results.

**Table I. Characteristics and Investigator Global Assessment of Rosacea Severity Score (IGA-RSS) scores of the patient at each visit**

| | Baseline (n = 36) | Week 3 (n = 36) | p-value (vs baseline) | Week 6 (n = 36) | p-value (vs baseline) |
|---|---|---|---|---|---|
| TEWL, mean±SD | 16.16±5.15 | 15.41±4.14 | 0.305 | 14.56±5.23 | 0.079 |
| SSH, mean±SD | 47.80±20.07 | 59.05±16.22 | < 0.001 | 55.96±14.98 | 0.012 |
| Skin pH, mean±SD | 6.07±0.49 | 5.88±0.46 | 0.076 | 6.03±0.55 | 0.785 |
| EI, mean±SD | 354.3±89.6 | 358.1±77.3 | 0.754 | 327.7±75.4 | 0.031 |
| (CM2600D) a*, mean±SD | 11.78±2.28 | 11.30±2.85 | 0.288 | 10.83±2.79 | 0.023 |
| IGA-RSS grade, n (%) | | | | | |
| 1 | | 1 (2.78) | < 0.001 | 7 (19.44) | < 0.001 |
| 2 | | 9 (25.00) | | 13 (36.11) | |
| 3 | 15 (41.67) | 15 (41.67) | | 12 (33.33) | |
| 4 | 13 (36.11) | 9 (25.00) | | 4 (11.11) | |
| 5 | 8 (22.22) | 2 (5.56) | | | |

SD: standard deviation; TEWL: transepidermal water loss; SSH: skin surface hydration; EI: Erythema Index; the parameters were tested using the paired $t$-test.

## RESULTS

### Demographics of the patients with rosacea

A total of 41 patients with rosacea were enrolled, and 36 completed the treatment. The mean age of the 36 patients was $37.25 \pm 8.18$ years. Among the 36 participants, 55.6% achieved "treatment success". The characteristics are shown in **Table I**. Only 3 participants had treatment-related AEs (all were mild or moderate), including dizziness, stomach ache, and diarrhoea.

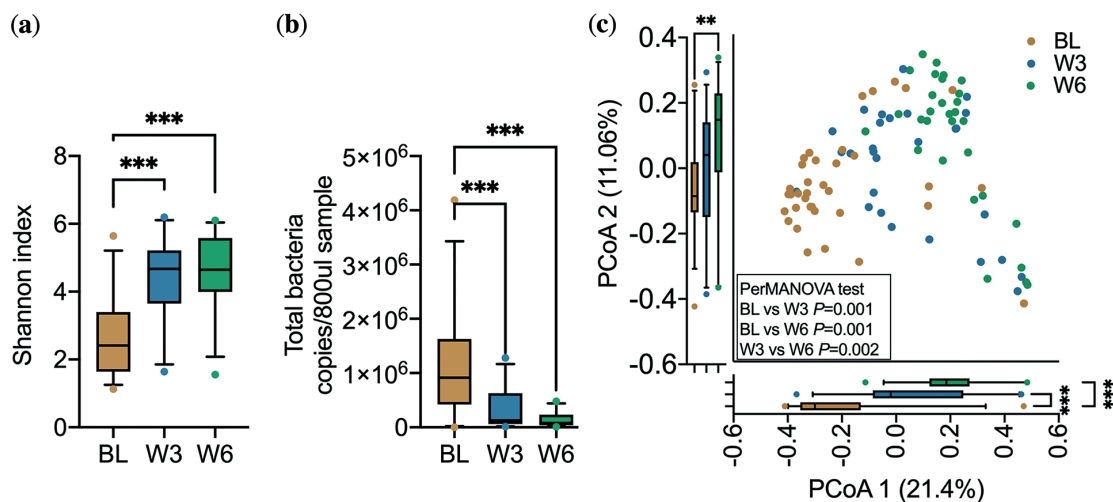### Alpha-diversity and structure of the skin microbiota

A total of 113 skin samples were obtained (18 samples were excluded for insufficient DNA), and 95 samples were sequenced for 16S rRNA V3–V4 gene analysis. The Shannon index (median at baseline 2.412; inter-quartile range (IQR) 1.644–3.395; median at 6 weeks 4.649; IQR 3.991–5.582; $p<0.001$) and the observed ASVs number (median at baseline 71.0; IQR 45.5–109.5; median at 6 weeks 151.5; IQR 97.8–189.8; $p<0.001$) of the skin microbiota were increased 1.74-fold and 1.77-fold, respectively, after the treatment (6 weeks) (**Fig. 1**a). The total number of bacteria on the skin decreased after the treatment (median at baseline 5.962; IQR, 5.650–6.237; median at 3 weeks 5.156; IQR 4.811–5.873; median at 6 weeks 5.277; IQR 4.660–5.458) (Fig. 1b). PCoA based on the Bray Curtis distances between the samples was applied to show the changes in microbial structure (Fig. 1c). The PerMANOVA test showed that the shift of microbiota structure was distinct during the minocycline treatment.

### Variation in taxonomic composition of skin microbiota

Based on the amplicon sequencing data, 282 families and 572 genera were annotated. This study identified 94, and 80 genera changed at week 3 or week 6 compared with baseline using the LEfSe model. Finally, 40 genera were confirmed as the key genera that varied notably and commonly at week 3 or 6 compared with baseline (**Fig. 2**a). Compared with baseline, the mean relative abundance of *Cutibacterium* and *Staphylococcus* were both decreased 2.23-fold (log₂-transformed, similarly hereinafter) and 1.79-fold, respectively, at week 3 (*Cutibacterium*, FDR-adjusted $p = 0.0028$; *Staphylococcus*, FDR-adjusted



**Fig. 1. Changes in skin bacterial diversity, amount, and structure after treatment.** (a) Variations in α-diversity indexes Shannon index. (b) Variation in total bacteria copies in skin samples. (c) Variation in the structure of skin microbiota. Principal coordinates analysis (PCoA) was performed based on the Bray Curtis distance, and PerMANOVA test results are shown in the lower left of the PCoA plot. Sample sites on the PCoA axis 1 and PCoA axis 2 were shown as the box-plots. For the box-plot, the horizontal bar within box-plots represents the median; bottom and top of each box, first and third quartiles; the lower error bar extends to the 5th percentile of the data; the upper error bar extends to the 95th percentile of the data. Data points beyond the 95th percentile or below the 5th percentile were plotted individually as outliers. Kruskal–Wallis test with Dunn's multiple comparisons was used to evaluate the difference between the 3 time-points. **$p < 0.01$, ***$p < 0.001$. BL: baseline; W3: 3 weeks after treatment; W6: 6 weeks after treatment.

$p=0.016$), and the relative abundance of *Cutibacterium* decreased 3.045-fold further at week 6 (FDR-adjusted $p<0.001$). *Clostridium* (increased 2.84-fold, FDR-adjusted $p=0.0028$), *Brachybacterium* (increased 1.96-fold, FDR-adjusted $p=0.017$), *Bdellovibrio* (increased 4.66-fold, FDR-adjusted $p=0.005$), *Xanthomonas* (increased 4.66-fold, FDR-adjusted $p=0.005$), were enriched notably at week 3. Moreover, the mean relative abundance of *Clostridium* (increased 2.73-fold, FDR-adjusted $p=0.03$), *Bdellovibri* (increased 2.63-fold, FDR-adjusted $p=0.036$), and *Xanthomonas* (increased 2.04-fold, FDR-adjusted $p=0.05$) kept higher than baseline, but slightly lower than week 3 (no statistically significant difference). The mean relative abundance of *Megasphaera* (increased 6.43-fold,

FDR-adjusted $p=0.038$) and *Roseburia* (increased 4.85-fold, FDR-adjusted $p=0.043$) increased significantly compared with baseline.

Eight patients with 24 samples from 3 time-points were randomly selected to perform the metagenomic sequencing to assess the changes in microbial composition at the species level. Then, the absolute abundance of each species was calculated from 21 samples of 7 patients because the total bacteria counts copies of these samples have been determined. The results are shown in Fig. 2b. The mean absolute abundance of *Cutibacterium acnes* decreased from baseline to week 3 (difference $-1.36\times10^{5}$; $p=0.08$) and further decreased at week 6 (difference $-1.52\times10^{5}$; $p=0.048$). The mean
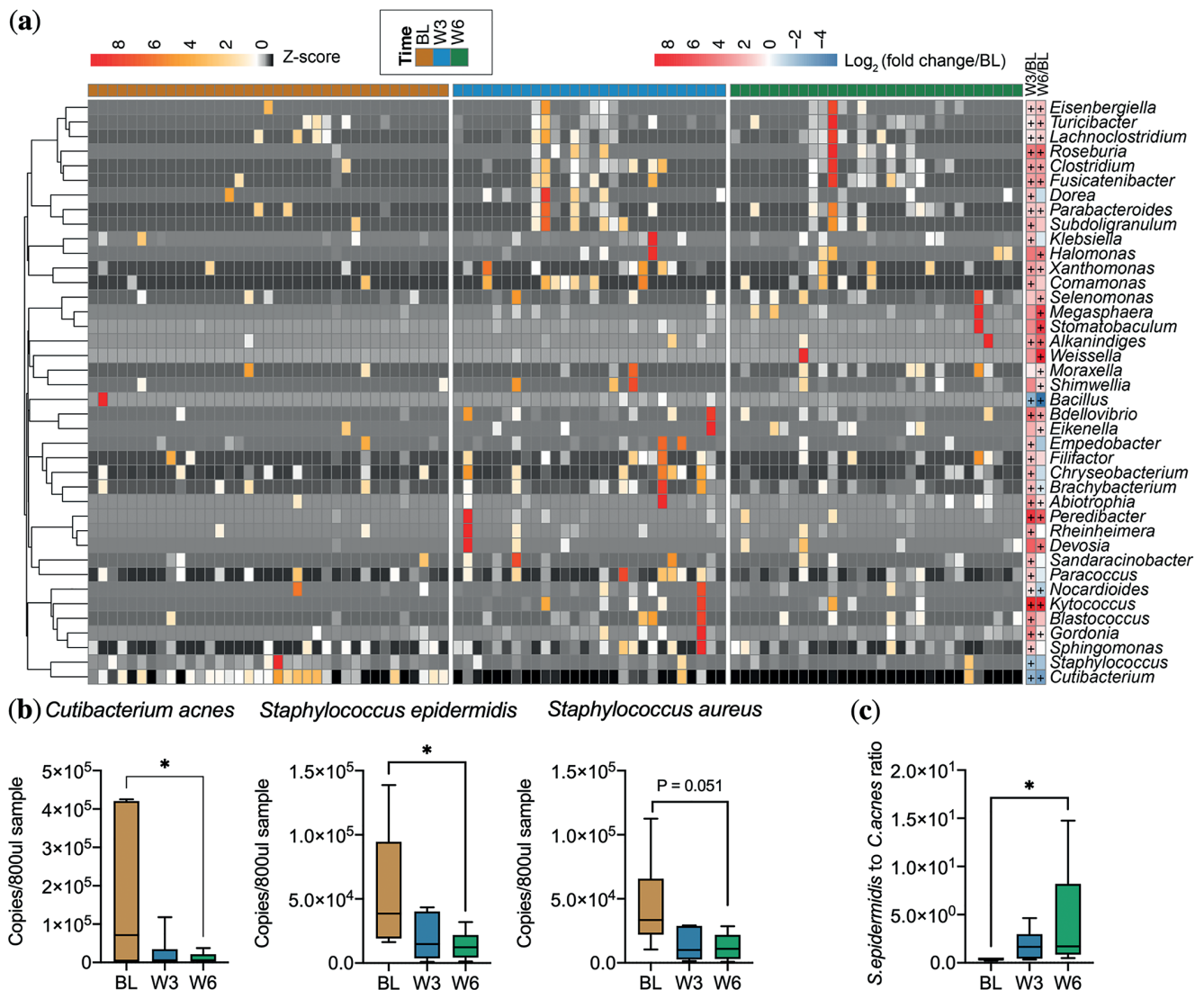


**Fig. 2. Changes in the composition of the skin microbiota during minocycline treatment.** (a) A total of 40 key genera were identified following treatment on amplicon sequencing. (b) Changes in the absolute abundances of *Cutibacterium acnes*, *Staphylococcus epidermidis,* and *Staphylococcus aureus* based on metagenomic sequencing data. (c) The ratio of the absolute abundance of *S. epidermidis* to *C. acnes*. For the heatmap in (a) the cluster of the amplicon sequence variants (ASVs) or genera based on Spearman's correlation coefficients is shown on the left. The heatmap in the middle shows the Z-score of each genus in individual samples at different time-points during treatment. The changes in the genera are shown on the righhand columns of the heatmap, + means false discovery rate (FDR)-adjusted $p<0.05$. For data in (b) the Kruskal–Wallis test with Dunn's multiple comparisons was used to evaluate the difference among the 3 time-points. For data in (c) a 1-way analysis of variance (ANOVA) test followed by Tukey's multiple comparisons was used to analyse the variations among groups. $*p<0.05$. BL: baseline; W3: 3 weeks after treatment; W6: 6 weeks after treatment.

absolute abundance of *Staphylococcus epidermidis* and *Staphylococcus aureus* was reduced from baseline to week 3 (*S. epidermidis* difference $-4.27 \times 10^5$; $p = 0.052$; *S. aureus* difference $-3.06 \times 10^5$; $p = 0.054$). The mean absolute abundance of *S. epidermidis* showed a significant reduction at week 6 (difference $-4.65 \times 10^5$; $p = 0.04$), while the mean absolute abundance of *S. aureus* kept a lower, but not significantly different, level (difference $-3.22 \times 10^5$; $p = 0.051$) compared with baseline. Although both the absolute abundance of *S. epidermidis* and *C. acnes* decreased following treatment, the ratio of the absolute abundance of *S. epidermidis* to *C. acnes* was significant from baseline to week 6 (difference 3.88; $p = 0.027$) (Fig. 2c).

*Variation in metabolic functions of skin microbiota*

Seventy-nine metabolic pathways were identified as the key pathways that were enriched notably at week 3 or 6 compared with baseline, and 45 top-fold change pathways were shown in **Fig. 3**a. Among these pathways, various pathways were related to the meta-cleavage degradation of aromatic compounds. For example, at week 6, the relative abundance of L-tryptophan degradation IX pathway (increased 2.26-fold; FDR-adjusted $p < 0.001$), L-tryptophan degradation to 2-amino-3-carboxymuconate semialdehyde (increased 3.46-fold; FDR-adjusted $p < 0.001$), catechol degradation I (increased 2.48-fold; FDR-adjusted $p < 0.001$), and toluene degradation I (increased 2.21-fold; FDR-adjusted $p < 0.001$) were higher than baseline. In order to verify the results, the microbial whole genomes were annotated in 21 samples of 7 patients to the KEGG database, then evaluated the changes in gene abundance related to different metabolic functions over time at the module level (Fig. 3b). Following treatment, the modules where tryptophan was broken down to 2-aminomuconate (week 3 to baseline difference 0.089%; $p = 0.008$; week 6 to baseline difference 0.081%; $p = 0.04$) or nicotinamide adenine dinucleotide (NAD) (week 6 to baseline difference, 0.13%; $p = 0.02$) were both enriched. In addition, the toluene degradation module (difference 0.007%; $p = 0.026$) and catechol meta-cleavage module (difference 0.04%; $p = 0.049$) was enriched after 6 weeks. The mean abundance of the crucial genes related to the microbial butyrate synthesis was also higher than the baseline, based on the metagenomic sequences (*4hbt*, difference 403.7; $p = 0.039$; *atoD*, difference 163.82, $p = 0.038$) (Fig. 3c).

*Correlations of microbial composition, metabolic functions, and clinical parameters*

Spearman's correlation analyses were performed among the key genera, key metabolic pathways and clinical parameters (**Fig. 4**). *Cutibacterium* and *Staphylococcus* were negatively correlated with almost all the varied pathways related to aromatic compound degradation and butyrate synthesis. The pathway related to butyrate synthesis (PWY-5676) was positively correlated with skin surface hydration (SSH) ($\rho$ 0.22; FDR-adjusted $p = 0.099$), negatively correlated with EI ($\rho$ $-0.2$; FDR-adjusted $p = 0.099$) and IGA-RSS score ($\rho$ $-0.53$; FDR-adjusted $p < 0.001$). *Cutibacterium* and *Staphylococcus* showed negative connections with the SSH (*Cutibacterium* $\rho$ $-0.25$; FDR-adjusted $p = 0.04$; *Staphylococcus* $\rho$ $-0.28$; FDR-adjusted $p = 0.017$) and positive connections with IGA-RSS score (*Cutibacterium* $\rho$ 0.47; FDR-adjusted $p < 0.001$; *Staphylococcus* $\rho$ 0.37; FDR-adjusted $p = 0.002$). The abundance of *Megasphaera* showed negative correlations with TEWL ($\rho$ $-0.25$; FDR-adjusted $p = 0.020$), EI ($\rho$ $-0.32$; FDR-adjusted $p = 0.006$), (CM2600D) a* ($\rho$ $-0.26$; FDR-adjusted $p = 0.019$), and IGA-RSS score ($\rho$ $-0.34$; FDR-adjusted $p = 0.006$).

*Antibiotic resistance*

The gene abundance related to tetracycline resistance increased with time (median at baseline 0.0075; IQR 0.004–0.018; median at 3 weeks after treatment (W3) 0.009; IQR 0.003–0.027; median at 6 weeks after treatment (W6) 0.02; IQR 0.016–0.093) (**Fig. 5**a). Meanwhile, the gene abundance related to multidrug resistance also increased with time (median at baseline 0.198; IQR 0.094–0.618; median at W3 0.611; IQR 0.323–0.905; median at W6 0.641; IQR 0.515–0.964) (Fig. 5b).

## DISCUSSION

The microbiota plays the important role of a barrier with protective roles, including physical skin barrier differentiation and epithelialization (23). The current study suggests that minocycline significantly changed the diversity and overall microbiota structure of the skin microbiome of patients with rosacea. The total number of skin bacteria decreased, but the species diversity increased. Thus, the key to skin disease or protection lies in the steady state of bacterial diversity. After the homeostasis of the skin microbial communities is destroyed, every bacterium may be suspected of being pathogenic.

A few sequencing-based studies have investigated the changes in skin microbiota populations after systemic antibiotics, reporting a negligible effect of antibiotics on the skin microbiome (24–26). In the current study, the abundance of *C. acnes* and *S. epidermidis* on the skin decreased significantly after oral minocycline treatment. Among all subtypes of rosacea, the most abundant species is consistently *C. acnes* (27), supporting the current study, which showed that *C. acnes* was the most dominant species at baseline, followed by *S. epidermidis*. After 6 weeks of treatment, the 2 positions reversed. Conversely, culture-based studies showed long-term alterations of the commensal skin microbiota by antibiotics, with decreasing numbers of commensal *Staphylococcus*
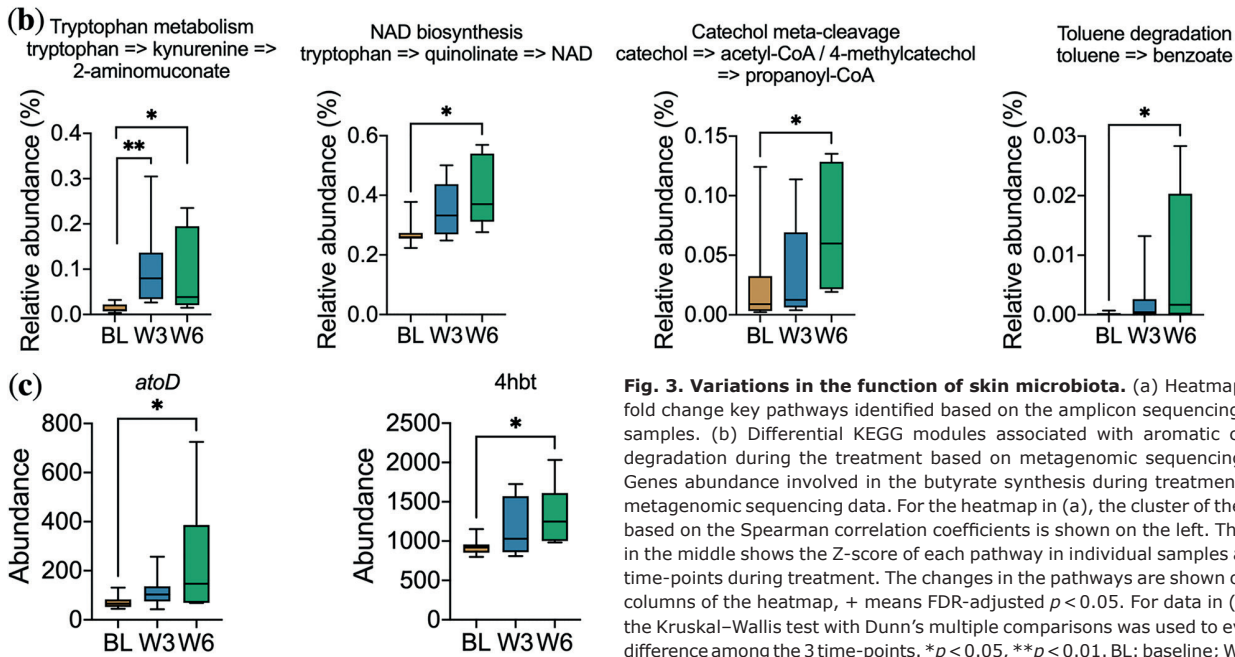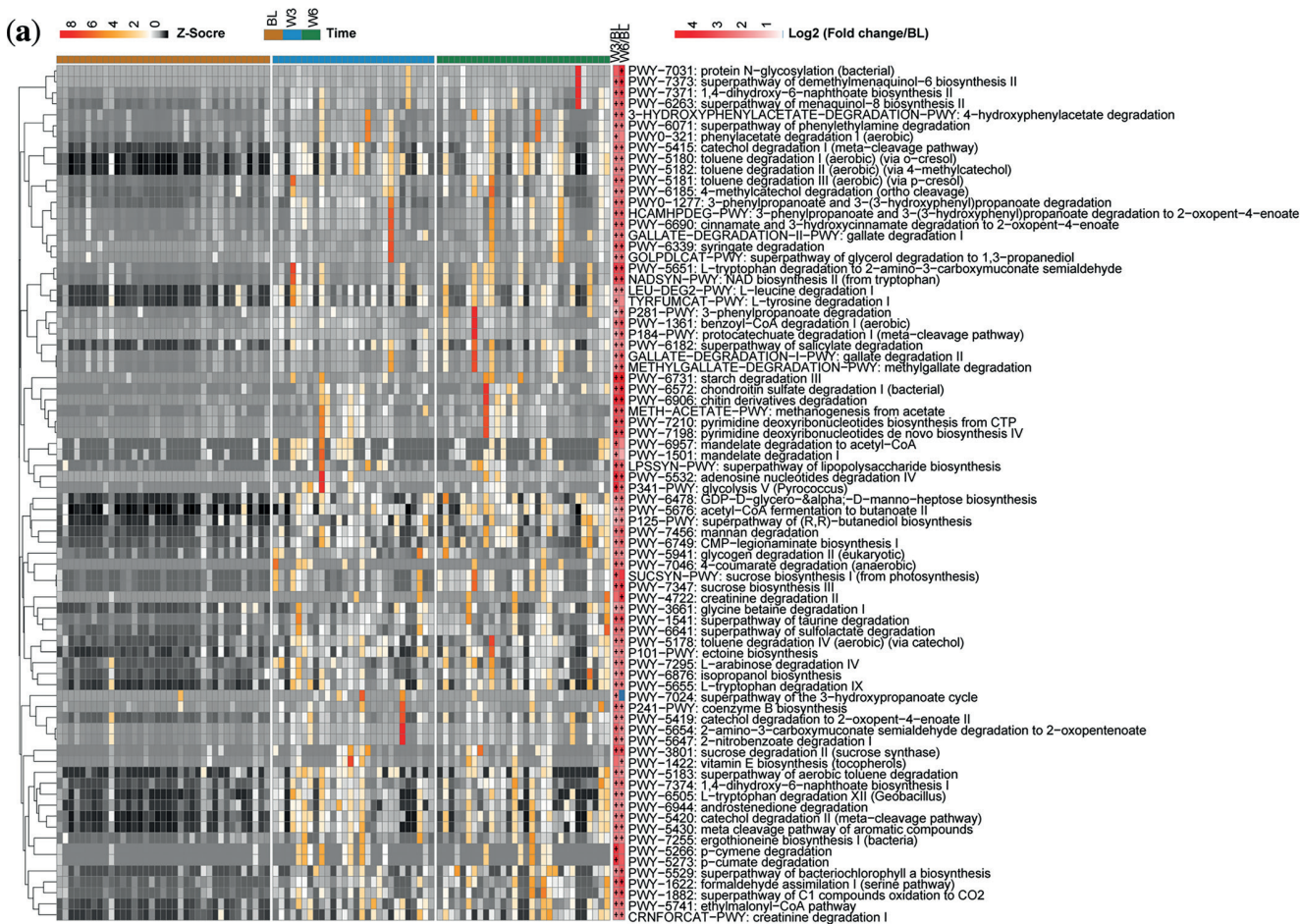
**Fig. 3. Variations in the function of skin microbiota.** (a) Heatmap of 45 top fold change key pathways identified based on the amplicon sequencing of all skin samples. (b) Differential KEGG modules associated with aromatic compounds degradation during the treatment based on metagenomic sequencing data. (c) Genes abundance involved in the butyrate synthesis during treatment based on metagenomic sequencing data. For the heatmap in (a), the cluster of the pathways based on the Spearman correlation coefficients is shown on the left. The heatmap in the middle shows the Z-score of each pathway in individual samples at different time-points during treatment. The changes in the pathways are shown on the right columns of the heatmap, + means FDR-adjusted $p < 0.05$. For data in (b) and (c), the Kruskal–Wallis test with Dunn's multiple comparisons was used to evaluate the difference among the 3 time-points. *$p < 0.05$, **$p < 0.01$. BL: baseline; W3: 3 weeks after treatment; W6: 6 weeks after treatment; 4hbt, butyryl-CoA: 4-hydroxybutyrate CoA transferase; atoD, butyryl-CoA: acetoacetate CoA transferase beta subunit.
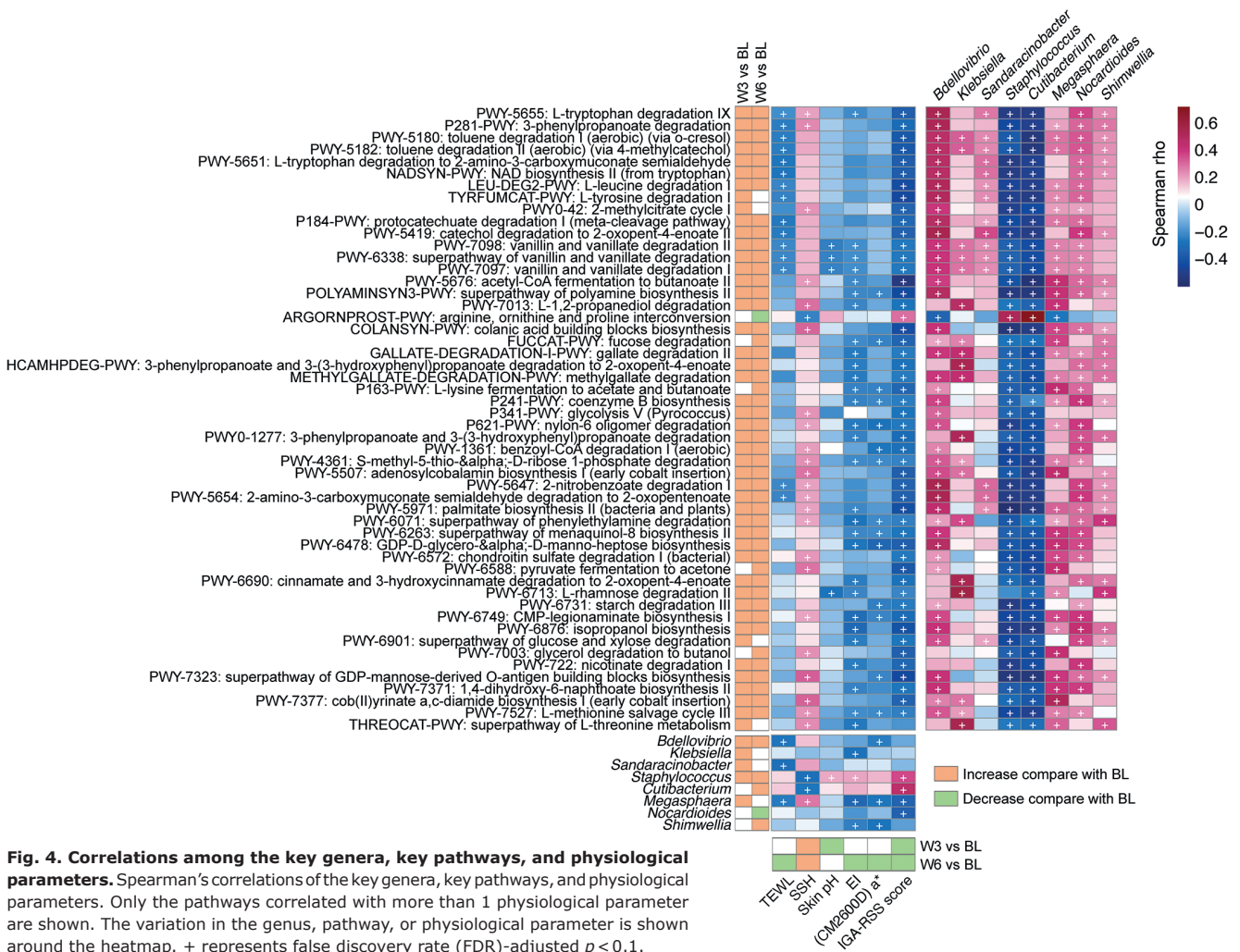
**Fig. 4. Correlations among the key genera, key pathways, and physiological parameters.** Spearman's correlations of the key genera, key pathways, and physiological parameters. Only the pathways correlated with more than 1 physiological parameter are shown. The variation in the genus, pathway, or physiological parameter is shown around the heatmap. + represents false discovery rate (FDR)-adjusted $p < 0.1$.
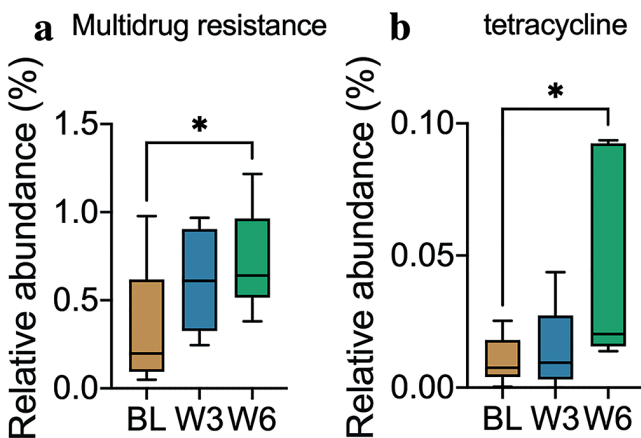


**Fig. 5. Variations in bacterial antibiotic resistance.** (a) Bacterial gene relative abundance related to tetracycline resistance. (b) Bacterial gene relative abundance related to multidrug resistance pathways. Kruskal–Wallis test with Dunn's multiple comparisons was used to evaluate the difference among the 3 time-points, *$p < 0.05$. BL: baseline; W3: 3 weeks after treatment; W6: 6 weeks after treatment.

and *Cutibacterium* bacteria and increasing numbers of antibiotic-resistant microbes (28–31).

Skin microbiota can regulate epithelial differentiation and barrier function in stratified epithelia through the aryl hydrocarbon receptor (32). In the current study, the abundance of key genes in butyrate synthesis and tryptophan catabolism pathways increased after minocycline treatment, indicating that butyrate and tryptophan metabolites increased, which would be conducive to inhibiting skin inflammation and promoting barrier repair. Butyrate synthesis and aromatic compound catabolic pathway were negatively correlated with TEWL, skin pH, skin blood flow, and EI and positively correlated with SSH. These results suggest that increased butyrate and aromatic compound catabolites promote skin barrier repair, increase cuticle water content, and reduce facial flushing due to inflammation.

This study used metagenomic sequencing to identify antibiotic resistance genes in the skin's microbiota, revealing an increase in resistance, including multidrug and tetracycline resistance, following minocycline treatment. This can lead to an increase in antibiotic-resistant skin

microbes over time and potentially spread these resistant microbes to the broader population through skin shedding (33–35). Subtherapeutic antibiotic doses, such as doxycycline 20 mg, have been shown to exert weaker selection pressure for the emergence of drug-resistant bacteria compared with higher doses (36). As a potential alternative, low-dose doxycycline (20 mg twice daily) is suggested (37). There are currently no FDA-approved topical probiotics for rosacea, due to insufficient large-scale effectiveness data and understanding of side-effects. This study proposes microbial metabolites, such as butyrate and tryptophan metabolites, as potential therapeutic drugs, due to their precise and rapid action on target sites and lesser likelihood of causing side-effects.

In conclusion, this study suggests that the treatment of rosacea using minocycline leads to significant changes in the distribution of IGA scores, α-diversity, and microbiota structure. Treatment increased bacterial metabolic pathways like butyrate synthesis and L−tryptophan degradation, which would be conducive to inhibiting skin inflammation and promoting skin barrier repair. In addition, tetracycline and multidrug resistance increased after treatment.

## ACKNOWLEDGEMENTS

## REFERENCES

1. van Zuuren EJ. Rosacea. N Engl J Med 2017; 377: 1754–1764.
2. Wilkin J. Updating the diagnosis, classification and assessment of rosacea by effacement of subtypes. Br J Dermatol 2017; 177: 597–598.
3. Bakar O, Demircay Z, Toker E, Cakir S. Ocular signs, symptoms and tear function tests of papulopustular rosacea patients receiving azithromycin. J Eur Acad Dermatol Venereol 2009; 23: 544–549.
4. Vieira AC, Mannis MJ. Ocular rosacea: common and commonly missed. J Am Acad Dermatol 2013; 69: S36–41.
5. Two AM, Wu W, Gallo RL, Hata TR. Rosacea: part I. Introduction, categorization, histology, pathogenesis, and risk factors. J Am Acad Dermatol 2015; 72: 749–758; quiz 759–760.
6. Steinhoff M, Schauber J, Leyden JJ. New insights into rosacea pathophysiology: a review of recent findings. J Am Acad Dermatol 2013; 69: S15–26.
7. Wang R, Farhat M, Na J, Li R, Wu Y. Bacterial and fungal microbiome characterization in patients with rosacea and healthy controls. Br J Dermatol 2020; 183: 1112–1114.
8. Holmes AD. Potential role of microorganisms in the pathogenesis of rosacea. J Am Acad Dermatol 2013; 69: 1025–1032.
9. Kim HS. Microbiota in Rosacea. Am J Clin Dermatol 2020; 21: 25–35.
10. Dahl MV, Ross AJ, Schlievert PM. Temperature regulates bacterial protein production: possible role in rosacea. J Am Acad Dermatol 2004; 50: 266–272.
11. Thiboutot D, Anderson R, Cook-Bolden F, Draelos Z, Gallo RL, Granstein RD, et al. Standard management options for rosacea: the 2019 update by the National Rosacea Society Expert Committee. J Am Acad Dermatol 2020; 82: 1501–1510.
12. Tsianakas A, Pieber T, Baldwin H, Feichtner F, Alikunju S, Gautam A, et al. Minocycline extended-release comparison with doxycycline for the treatment of rosacea: a randomized, head-to-head, clinical trial. J Clin Aesthet Dermatol 2021; 14: 16–23.
13. Martins AM, Marto JM, Johnson JL, Graber EM. A review of systemic minocycline side effects and topical minocycline as a safer alternative for treating acne and rosacea. Antibiotics (Basel) 2021; 10: 757.
14. Jackson JM, Kircik LH, Lorenz DJ. Efficacy of extended-release 45 mg oral minocycline and extended-release 45 mg oral minocycline plus 15% azelaic acid in the treatment of acne rosacea. J Drugs Dermatol 2013; 12: 292–298.
15. Thompson KG, Rainer BM, Antonescu C, Florea L, Mongodin EF, Kang S, et al. Minocycline and its impact on microbial dysbiosis in the skin and gastrointestinal tract of acne patients. Ann Dermatol 2020; 32: 21–30.
16. Xu H, Li H. Acne, the skin microbiome, and antibiotic treatment. Am J Clin Dermatol 2019; 20: 335–344.
17. Moura IB, Grada A, Spittal W, Clark E, Ewin D, Altringham J, et al. Profiling the effects of systemic antibiotics for acne, including the narrow-spectrum antibiotic sarecycline, on the human gut microbiota. Front Microbiol 2022; 13: 901911.
18. Schaller M, Almeida LMC, Bewley A, Cribier B, Del Rosso J, Dlova NC, et al. Recommendations for rosacea diagnosis, classification and management: update from the global ROSacea COnsensus 2019 panel. Br J Dermatol 2020; 182: 1269–1276.
19. Bageorgou F, Vasalou V, Tzanetakou V, Kontochristopoulos G. The new therapeutic choice of tranexamic acid solution in treatment of erythematotelangiectatic rosacea. J Cosmet Dermatol 2019; 18: 563–567.
20. Klindworth A, Pruesse E, Schweer T, Peplies J, Quast C, Horn M, et al. Evaluation of general 16S ribosomal RNA gene PCR primers for classical and next-generation sequencing-based diversity studies. Nucleic Acids Res 2013; 41: e1.
21. Bolyen E, Rideout JR, Dillon MR, et al. Reproducible, interactive, scalable and extensible microbiome data science using QIIME 2. Nat Biotechnol 2019; 37: 852–857.
22. Douglas GM, Maffei VJ, Zaneveld JR, et al. PICRUSt2 for prediction of metagenome functions. Nat Biotechnol 2020; 38: 685–688.
23. Woo YR, Lim JH, Cho DH, Park HJ. Rosacea: molecular mechanisms and management of a chronic cutaneous inflammatory condition. Int J Mol Sci 2016; 17: 1562.
24. Naik S, Bouladoux N, Wilhelm C, Molloy MJ, Salcedo R, Kastenmuller W, et al. Compartmentalized control of skin immunity by resident commensals. Science 2012; 337: 1115–1119.
25. Abeles SR, Jones MB, Santiago-Rodriguez TM, Ly M, Klitgord N, Yooseph S, et al. Microbial diversity in individuals and their household contacts following typical antibiotic courses. Microbiome 2016; 4: 39.
26. Zhang M, Jiang Z, Li D, Jiang D, Wu Y, Ren H, et al. Oral antibiotic treatment induces skin microbiota dysbiosis and influences wound healing. Microb Ecol 2015; 69: 415–421.
27. Rainer BM, Thompson KG, Antonescu C, Florea L, Mongodin EF, Bui J, et al. Characterization and analysis of the skin microbiota in rosacea: a case-control study. Am J Clin Dermatol 2020; 21: 139–147.
28. Brown JM, Poston SM. Resistance of propionibacteria to antibiotics used in the treatment of acne. J Med Microbiol 1983; 16: 271–280.
29. Kurokawa I, Nishijima S, Asada Y. The antibiotic susceptibility of Propionibacterium acnes: a 15-year bacteriological study and retrospective evaluation. J Dermatol 1988; 15: 149–154.
30. Marples RR, Kligman AM. Ecological effects of oral antibio-

tics on the microflora of human skin. Arch Dermatol 1971; 103: 148–153.

31. Eady EA, Cove JH, Holland KT, Cunliffe WJ. Superior antibacterial action and reduced incidence of bacterial resistance in minocycline compared with tetracycline-treated acne patients. Br J Dermatol 1990; 122: 233–244.

32. Uberoi A, Bartow-McKenney C, Zheng Q, Flowers L, Campbell A, Knight SAB, et al. Commensal microbiota regulates skin barrier function and repair via signaling through the aryl hydrocarbon receptor. Cell Host Microbe 2021; 29: 1235–1248.e8.

33. Lax S, Smith DP, Hampton-Marcell J, Owens SM, Handley KM, Scott NM, et al. Longitudinal analysis of microbial interaction between humans and the indoor environment. Science 2014; 345: 1048–1052.

34. Hsu T, Joice R, Vallarino J, Abu-Ali G, Hartmann EM, Shafquat A, et al. Urban transit system microbial communities differ by surface type and interaction with humans and the environment. mSystems 2016; 1: e00018-16.

35. Weiss H, Hertzberg VS, Dupont C, Espinoza JL, Levy S, Nelson K, et al. The airplane cabin microbiome. Microb Ecol 2019; 77: 87–95.

36. Jo JH, Harkins CP, Schwardt NH, Portillo JA, Program NCS, Zimmerman MD, et al. Alterations of human skin microbiome and expansion of antimicrobial resistance after systemic antibiotics. Sci Transl Med 2021; 13: eabd8077.

37. Walker C, Preshaw PM, Novak J, Hefti AF, Bradshaw M, Powala C. Long-term treatment with sub-antimicrobial dose doxycycline has no antibacterial effect on intestinal flora. J Clin Periodontol 2005; 32: 1163–1169.